Structural cooperativity in the SH3 domain studied by site-directed mutagenesis and amide hydrogen exchange

S. Casares, M. Sadqi, O. López-Mayorga, J.C. Martínez, F. Conejero-Lara*

Departamento de Química Física e Instituto de Biotecnología, Facultad de Ciencias, Universidad de Granada, 18071 Granada, Spain

Received 2 December 2002; revised 22 January 2003; accepted 27 January 2003

First published online 5 March 2003

Edited by Thomas L. James

Abstract **We have studied the effects produced by site-directed mutagenesis upon energetic and structural cooperativity in the Src homology region 3 domain of α-spectrin. The mutation of Asn47 to Gly or Ala in the distal loop brings about significant changes to the global stability of the domain in spite of not affecting its structure to any great extent. The binding affinity for a proline-rich peptide is also largely diminished in both mutant domains. We have compared the apparent Gibbs energies of the amide hydrogen–deuterium exchange (HX) between the wild-type and the Gly47 mutant. The observed changes in the Gibbs energy of HX indicate a remarkable energetic cooperativity in this small domain. Regions of the domain's core have a high cooperativity with the position of the mutation, indicating that their HX occurs mainly in states in which the distal loop is unstructured. More flexible regions, which undergo HX mainly by local motions, show a lower but still considerable cooperativity with the distal loop. We conclude that there is an important correlation between regional stability and cooperativity in this small domain.**

Key words: Amide hydrogen–deuterium exchange; Nuclear magnetic resonance; Src homology region 3 domain; Protein folding; Protein stability; Structural cooperativity; Calorimetry

1. Introduction

There is increasing evidence, mainly from nuclear magnetic resonance (NMR)-detected amide hydrogen–deuterium exchange (HX), that proteins must be regarded not as simple cooperative units but rather as complex statistical ensembles of conformational states [1–10]. The patterns of HX protection under native conditions indicate that protein structures fluctuate in such a way that many amide groups are exposed to the solvent as a result of local or sub-global unfolding events. This statistical nature of proteins has been proposed as a key feature in explaining phenomena such as long-range cooperativity and allosteric regulation [11–13], and there is also increasing evidence to support the connection between folding and functional cooperativity in proteins [14].

Src homology region 3 (SH3) domains are small homologous modules that mediate protein–protein interactions in a variety of cellular processes [15]. The SH3 domain of α-spectrin is a small domain of 62 residues, which folds and unfolds in an apparent two-state reaction [16]. Analysis by mutagenesis of the folding–unfolding reactions of this and other homologous SH3 domains has indicated that their transition-state ensembles of folding are quite defined and conformationally restricted [17–19]. The largest *phy* factors of the α-spectrin SH3 domain occur in the distal β-hairpin and the short 3_{10} helix, indicating that these regions are mainly folded in the transition state. Mutations made at positions 47 and 48 of SH3, at the tip of the distal loop (a type II′ β-turn), have a significant effect upon the stability of the domain, apparently due to changes in the local conformational strain existing at position 47 [17,20]. In particular, Asn47 has ϕ and ψ angles only allowed to Gly in the Ramachandran plot [21]. Mutations of Asn47 to Gly or Ala (N47G, N47A), however, cause smaller stability changes than might initially be expected [20].

We have shown in previous papers that, in spite of the apparent two-state character of the SH3 folding reaction, under native conditions the HX of SH3 is governed by a variety of conformational states, which range from local fluctuations affecting the loops and chain ends to large structural disruptions involving most of the structure of the domain [9,22,23]. By analysing the effect of pH and temperature on HX from a statistical–thermodynamic point of view we have deduced average thermodynamic and structural properties for these conformational states [22,23].

Given the large amount of data available concerning the folding and conformational stability of the SH3 domain, this system would appear to be ideal for exploring the relationship between structural and functional cooperativity and folding. The importance of the distal loop in the folding and global stability of the SH3 domain has led us to explore the effect of changing the local stability at the distal loop upon the cooperativity of this small domain. In this work we report on the effect of site-directed mutagenesis at position 47 upon HX in the SH3 domain under native conditions.

2. Materials and methods

The DNA encoding the mutant SH3 domains (N47A and N47G) was obtained by polymerase chain reaction [24]. The wild-type (WT) and mutant proteins were isolated as described elsewhere [9].

*Corresponding author. Fax: (34)-958-272879.
E-mail address: conejero@ugr.es (F. Conejero-Lara).

Abbreviations: SH3, Src homology region 3; HX, amide hydrogen–deuterium exchange; pH*, pH-meter reading for deuterium oxide solutions uncorrected for isotopic effects; WT, wild-type; N47G and N47A, single mutants of the SH3 domain of α-spectrin with asparagine 47 replaced by glycine and alanine respectively; p41, decapeptide of sequence APSYSPPPPP both acetylated and methylated in its N- and C-termini, respectively; DSC, differential scanning calorimetry

0014-5793/03/$22.00 © 2003 Published by Elsevier Science B.V. on behalf of the Federation of European Biochemical Societies.
doi:10.1016/S0014-5793(03)00212-6

Titration experiments monitoring the change in intensity of tryptophan fluorescence were carried out at both pH 3.0 and 7.0 to estimate the binding affinities of the SH3 variants for the decapeptide of sequence APSYSPPPPP both acetylated and methylated in its N- and C-termini, respectively (p41) [25]. Protein samples were maintained at 25°C by thermostat in the fluorimeter's cuvette at a concentration of ~25 μM. Fluorescence spectra were recorded between 300 and 400 nm at different p41 concentrations from 0 to ~1 mM. The excitation wavelength was 298 nm. The titration curves were analysed as described elsewhere [25].

NMR chemical shift assignment of the amide and α protons of the two mutant SH3 domains was performed using a set of COSY, TOCSY and NOESY experiments in 90% H_2O–10% D_2O at pH* (direct pH-meter reading for deuterium oxide solutions uncorrected for isotopic effects) 3.0 and 27.1°C. All NMR spectra were processed and analysed using NMRpipe [26] and NMRview [27].

NMR-detected HX experiments were made as described elsewhere [9] to determine the exchange rate constants, k_{ex}, for the WT and N47G SH3 domains in 20 mM d_5-glycine at pH* 3.0 and 27.1°C. The final protein concentration was about 4.5 mM. Intrinsic exchange rate constants for each amide proton, k_{int}, at pH* 3.0 were calculated for both protein sequences as described elsewhere [28]. An EX2 mechanism for HX was assumed under our experimental conditions [22]. The equilibrium constant, K_{op}, for the opening process, rendering the amide hydrogen of any particular residue susceptible to exchange, was calculated as being $K_{op} = k_{ex}/k_{int}$, and the apparent Gibbs energy of the exchange was obtained by $\Delta G_{ex} = -RT \cdot \ln K_{op}$.

Comparative computer analysis of the crystal structures of the three SH3 variants was made with WHATIF [29] using the PDB files 1SHG (WT) [21], 1QKW (N47G) and 1QKX (N47A) [20]. Structural alignments were performed both for the backbone atoms and for all the atoms of the proteins. Solvent-accessible surface areas (ASA) were calculated using a probe radius of 1.4 Å. The number of inter-residue atomic contacts was calculated for each variant as the number of inter-residue atom pairs at a distance equal to or lower than the sum of the van der Waals radii.

3. Results and discussion

The change in the Gibbs energy of global unfolding ($\Delta\Delta G_{unf}$) caused by the mutations at sequence position 47 was estimated by differential scanning calorimetry (DSC) under the same conditions as those of the HX experiments (Table 1). The mutant N47A was 1.9 kJ/mol less stable than the WT domain at pH 3.0 and 27.1°C, while the N47G mutant was 2.0 kJ/mol more stable than the WT protein under the same conditions. At pH 7.0 all proteins were more stable but the $\Delta\Delta G_{unf}$ values remained very similar. These results agree well with previously published ones obtained under similar conditions [20].

To investigate any structural changes induced by the mutations we measured the NMR chemical shifts of the amide and α protons of the three SH3 variants at pH 3.0 and 27.1°C. Fig. 1 shows the differences in chemical shift for the α hydrogens between each pair of SH3 variants. The biggest differences were observed for residues 47 (position of the mutation) and 48 at the tip of the distal loop (the type II′ β-turn). The chemical shifts of other residues adjacent to these were also considerably affected. The differences in chemical shift for the amide protons were in general larger but open to similar interpretation (not shown).

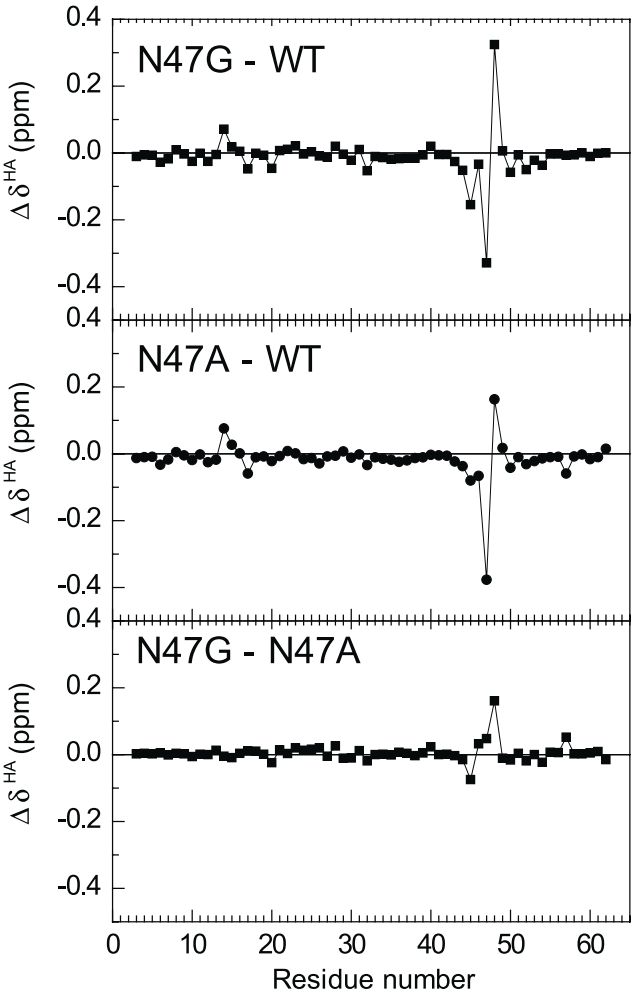

Fig. 1. Plot representing the differences in ^{1}H-NMR chemical shifts of the α protons between each pair of SH3 domain variants, as indicated in each panel.

Slight changes in the chemical shifts for D14 and E17 in the long RT loop could be detected when each mutant was compared to the WT protein, suggesting small, long-range structural changes induced by the removal of the polar group of N47. When both mutants were compared the differences in chemical shifts were almost negligible in most of the chain except around the distal loop. In this region the differences

Table 1
Thermodynamic parameters for the unfolding of WT and mutant SH3 domains at pH 3.0 and 7.0 as measured by DSC

	Protein	T_m (°C)	ΔH_{unf} (T_m) (kJ/mol)	$\Delta C_{p,unf}$ (50°C)[a] (kJ/K/mol)	ΔG_{unf} (27.1°C) (kJ/mol)	$\Delta\Delta G_{unf}$ (27.1°C) (kJ/mol)
pH 3.0	WT	55.2 ± 0.1	175 ± 1	2.94 ± 0.10	11.1 ± 0.2	–
	N47G	59.2 ± 0.1	186 ± 1		13.1 ± 0.2	2.0
	N47A	52.3 ± 0.1	160 ± 1		9.2 ± 0.3	−1.9
pH 7.0	WT	63.9 ± 0.1	212 ± 1	2.94 ± 0.10	17.2 ± 0.3	–
	N47G	66.6 ± 0.1	224 ± 1		19.4 ± 0.3	2.2
	N47A	61.9 ± 0.1	197 ± 1		15.0 ± 0.3	−2.2

The uncertainties in the parameters correspond to the standard errors of the fits using the two-state unfolding model.
[a]The heat capacity change of unfolding was fitted as a common parameter for all protein variants at each pH value.

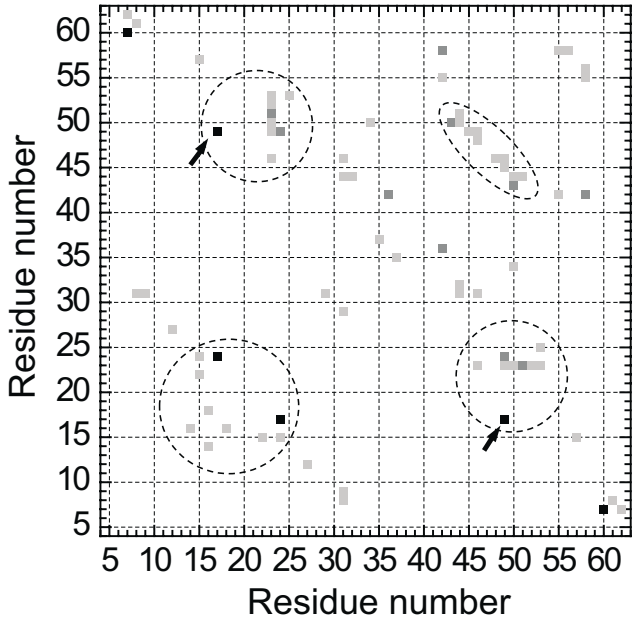

Fig. 2. Two-dimensional map showing the differences in the number of inter-residue atomic contacts between the crystal structures of the N47G mutant and the WT SH3 domains. The number of contacts gained or lost as a result of the mutation is indicated in grey scale: light grey, one contact; medium grey, two contacts; black, three or more contacts. Dashed lines highlight the regions of most significant changes. The arrows indicate the rupture of the salt bridge between E17 and R49 side chains.

were smaller than those found between each mutant and the WT domain. This indicates that the mutants are more similar to each other in structure than either is to the WT, suggesting a special role for the polar amide group of N47 in the changes observed.

We made a detailed comparative computer analysis of the crystal structures of the three SH3 variants. Their structural alignment indicates great similarity between the crystal structures of all the variants, with C_α–C_α distances slightly higher than average in the distal loop (results not shown). Nevertheless, all these distances (<0.5 Å) are significantly smaller than the resolution of the crystal structures (1.8–2.0 Å).

The ASAs of all three SH3 variants were compared (results not shown). The greatest changes caused by the N47G mutation were seen to occur in the distal loop and, to a lesser extent, in the RT loop. Significant changes were also observed for Leu34. Very similar differences in ASA values were observed between WT and N47A.

Inter-residue atomic-contact maps were compared for the three SH3 variants. Fig. 2 shows the difference in contacts between WT and N47G. In general the mutation causes minor changes to the number of inter-residue contacts in all the structural elements. The most significant of these occur in the distal β-hairpin, in the RT loop and in the contact region between them. The difference map for WT and N47A reveals similar features, whilst the map comparing the two mutant domains shows the lowest number of differences, which again indicates a higher structural similarity between the two mutants. Interestingly, the crystal structure of the WT protein shows a salt bridge between the side chain of R49 in the distal loop and that of E17 in the RT loop. This salt bridge is not present in any of the mutants' structures and appears to be stabilised by the interactions of the N47 side chain.

In conclusion, the only important changes to the crystal structure of the SH3 domain caused by the mutations at position 47 appear to consist of local effects around the distal loop. Possible long-range effects involve small rearrangements of inter-residue contacts, including the rupture of the E17–R49 salt bridge and perhaps some minor rearrangements within the RT loop.

We have monitored the effect of the Asn47 mutation upon the binding affinity of each SH3 variant for the ligand p41. This proline-rich decapeptide binds tightly to the Abl-SH3 domain compared with other peptides, due in part to favourable interactions with the RT loop [25]. Table 2 shows that p41 also binds with moderate affinity to the WT α-spectrin SH3 domain. Both mutations, N47A and N47G, positioned more than 10 Å from the binding site, produce a similar decrease in affinity, which supports the idea of a cooperative pathway between the distal loop and the binding site of the domain.

To explore further the cooperative pathways in the SH3 domain, we measured the HX of the N47G mutant at pH* 3.0 and compared it with the HX of the WT domain under the same conditions, which we have reported in a previous publication [9]. Table 3 includes the HX rate constants and the corresponding Gibbs energy values. The HX of N47A could not be measured under our experimental conditions due to protein aggregation. Fig. 3A shows a simplified scheme of the crystal structure of the WT domain, with the changes in apparent Gibbs energy of exchange, $\Delta\Delta G_{ex}$, caused by the mutation N47G indicated in grey-scale code. We have made a statistical–thermodynamic interpretation of the $\Delta\Delta G_{ex}$ values produced by a mutation in terms of probabilities of conformational ensembles of states, P_i [9,11,30,31].

A single-point mutation such as those studied here exerts a local energy perturbation that changes the probability of each state of the domain ensemble by a 'cooperativity factor' [11] given by

$$\phi_i = e^{-\Delta\Delta G_i/RT} \quad (1)$$

where $\Delta\Delta G_i = \Delta G_i^{mut} - \Delta G_i^{wt}$ represents the local Gibbs energy change in state i produced by the mutation.

Starting from the definition of the opening constant for a residue j, $K_{op,j}$, in terms of probabilities of states [9,11,30,31], the ratio between the opening constants of the mutant and the WT domains for residue j can be easily calculated as:

$$\frac{K_{op,j}^{mut}}{K_{op,j}^{wt}} = \frac{Q_{(j,ex)}^{-1} \cdot \sum_{i(j,ex)} \left(\phi_j \cdot e^{-\Delta G_i^{wt}/RT}\right)}{Q_{(j,nex)}^{-1} \cdot \sum_{i(j,nex)} \left(\phi_i \cdot e^{-\Delta G_i^{wt}/RT}\right)} = \frac{\langle\phi\rangle_{j,ex}}{\langle\phi\rangle_{j,nex}} \quad (2)$$

where ΔG_j^{wt} represents the Gibbs energy of each state of the

Table 2
Equilibrium dissociation constants of the complexes between the p41 peptide and the SH3 domain variants at pH 3.0 and 7.0 and at 25°C

	Protein	K_D (μM)
pH 3.0	WT	110 ± 30
	N47G	179 ± 19
	N47A	173 ± 18
pH 7.0	WT	83 ± 7
	N47G	125 ± 13
	N47A	131 ± 20

Table 3
HX rate constants and Gibbs energies of WT and N47G variants of SH3 at pH 3.0 and 27.1°C

Residue	WT		N47G	
	k_{ex}, $\times 10^3$ (min^{-1})	ΔG_{ex} (kJ/mol)	k_{ex}, $\times 10^3$ (min^{-1})	ΔG_{ex} (kJ/mol)
Leu8	9.0 ± 0.5	5.17 ± 0.14	6.65 ± 0.17	5.97 ± 0.06
Val9	1.11 ± 0.07	6.85 ± 0.15	0.52 ± 0.018	8.73 ± 0.09
Leu10	1.42 ± 0.07	7.14 ± 0.12	0.67 ± 0.08	9.0 ± 0.3
Ala11	2.15 ± 0.21	9.23 ± 0.25	0.90 ± 0.05	11.38 ± 0.14
Leu12	1.27 ± 0.07	8.36 ± 0.14	0.66 ± 0.06	10.00 ± 0.24
Tyr13	1.57 ± 0.04	8.33 ± 0.06	0.74 ± 0.04	10.21 ± 0.14
Asp14	20 ± 3	7.5 ± 0.4	18.0 ± 2.0	7.8 ± 0.3
Tyr15	4.5 ± 0.4	9.25 ± 0.22	2.4 ± 0.3	10.8 ± 0.3
Gln16	18.9 ± 1.2	5.18 ± 0.16	12.7 ± 0.5	6.24 ± 0.11
Glu17	–	–	15 ± 6	7.2 ± 0.9
Ser19	43 ± 8	5.3 ± 0.5	35 ± 11	5.9 ± 0.8
Glu22	20.6 ± 1.2	6.59 ± 0.15	12.1 ± 0.3	7.95 ± 0.06
Val23	4.90 ± 0.07	5.96 ± 0.04	2.67 ± 0.07	7.51 ± 0.07
Thr24	14.8 ± 0.7	3.97 ± 0.12	9.4 ± 0.4	5.18 ± 0.11
Met25	9.31 ± 0.4	7.31 ± 0.11	3.60 ± 0.12	9.73 ± 0.08
Lys26	10.1 ± 0.6	6.48 ± 0.15	6.0 ± 0.3	7.82 ± 0.12
Lys27	5.8 ± 2.3	8 ± 1	3.6 ± 1.4	9.1 ± 0.9
Gly28	11.5 ± 1.7	8.0 ± 0.4	–	–
Ile30	5.8 ± 0.3	5.98 ± 0.12	4.27 ± 0.11	6.77 ± 0.06
Leu31	1.30 ± 0.05	6.72 ± 0.11	0.65 ± 0.04	8.46 ± 0.17
Thr32	2.86 ± 0.12	7.65 ± 0.11	1.53 ± 0.11	9.27 ± 0.18
Leu33	2.20 ± 0.11	7.73 ± 0.12	0.94 ± 0.06	9.88 ± 0.16
Leu34	1.47 ± 0.17	6.9 ± 0.3	0.51 ± 0.04	9.53 ± 0.22
Asn35	5.6 ± 1.2	9.0 ± 0.5	3.5 ± 0.8	10.4 ± 0.5
Thr37	34 ± 4	4.4 ± 0.3	22.2 ± 1.6	5.50 ± 0.17
Asn38	24.3 ± 2.5	7.8 ± 0.3	16.5 ± 0.9	8.81 ± 0.13
Asp40	–	–	15.8 ± 1.6	8.5 ± 0.3
Trp41	6.04 ± 0.22	7.77 ± 0.09	3.88 ± 0.12	8.87 ± 0.08
Trp42	0.66 ± 0.05	10.02 ± 0.20	0.39 ± 0.05	11.4 ± 0.3
Lys43	1.86 ± 0.11	9.38 ± 0.14	0.82 ± 0.04	11.47 ± 0.13
Val44	1.22 ± 0.05	8.12 ± 0.11	0.52 ± 0.03	10.28 ± 0.13
Glu45	4.15 ± 0.09	8.52 ± 0.05	1.89 ± 0.08	10.50 ± 0.10
Val46	1.86 ± 0.11	8.32 ± 0.15	0.772 ± 0.024	10.54 ± 0.08
Arg49	10.4 ± 0.3	9.03 ± 0.07	6.97 ± 0.10	10.05 ± 0.04
Gln50	11.2 ± 0.3	7.38 ± 0.06	7.6 ± 0.3	8.44 ± 0.08
Gly51	8.0 ± 1.1	9.3 ± 0.3	4.1 ± 0.6	11.0 ± 0.3
Phe52	6.3 ± 0.3	7.10 ± 0.14	2.97 ± 0.16	8.99 ± 0.13
Val53	1.19 ± 0.05	7.81 ± 0.10	0.72 ± 0.08	9.1 ± 0.3
Ala55	2.7 ± 0.4	8.5 ± 0.4	1.48 ± 0.22	10.0 ± 0.4
Ala56	10.2 ± 0.9	6.51 ± 0.21	7.7 ± 0.5	7.24 ± 0.16
Tyr57	2.1 ± 0.1	8.75 ± 0.12	1.01 ± 0.05	10.56 ± 0.11
Val58	0.94 ± 0.03	8.36 ± 0.09	0.48 ± 0.04	10.06 ± 0.19
Lys59	2.76 ± 0.08	8.29 ± 0.07	1.25 ± 0.05	10.32 ± 0.09
Lys60	20 ± 4	4.8 ± 0.4	15.2 ± 2.5	5.6 ± 0.4
Leu61	8.7 ± 0.5	4.01 ± 0.14	6.3 ± 0.3	4.87 ± 0.11

conformational ensemble of the WT domain. The sums (j,ex) and (j,nex) are applicable to all the exchange-susceptible and non-exchange-susceptible states, respectively, for the amide group of residue j. $Q_{(j,ex)}$ and $Q_{(j,nex)}$ are the sub-partition functions for the exchange-susceptible and non-exchange-susceptible sub-ensembles, respectively. The fraction $\langle\phi\rangle_{j,ex}/\langle\phi\rangle_{j,nex}$ represents the average cooperativity factor for the sub-ensemble of states leaving residue j exposed to the solvent compared to the similar quantity for the sub-ensemble that buries the same residue. Finally, the increment in the Gibbs energy of HX produced by the mutation is given by:

$$\Delta\Delta G_{ex,j} = -RT \ln\left(\frac{K_{op,j}^{mut}}{K_{op,j}^{wt}}\right) = -RT \ln\frac{\langle\phi\rangle_{j,ex}}{\langle\phi\rangle_{j,nex}} \quad (3)$$

According to this equation, by measuring $\Delta\Delta G_{ex}$ we can estimate how a local energy perturbation, such as that produced by a single-point mutation, might change the average probability of the conformational sub-ensemble of states that leave each residue of the protein exposed to the solvent compared to the sub-ensemble of states that do not expose it.

The experimental data of $\Delta\Delta G_{ex}$ are represented in Fig. 3A. All residues with a measurable HX are affected to some extent by the mutation (see also Table 3), indicating a high energetic cooperativity in this small domain. This may be due to the intrinsically low stability of the domain (see Table 1), as has been discussed elsewhere from the results of computer simulations of cooperative interactions in proteins [11]. In addition, there are significant correlations between the $\Delta\Delta G_{ex}$ values and other previously reported magnitudes characterising the HX processes of SH3 [22,23], i.e. the average enthalpies, ΔH_{ex} (Fig. 3B), the average entropies and the average uptake of protons coupled to HX (not shown). This indicates that those regions of the domain undergoing larger structural motions show greater cooperative effects and vice versa.

The $\Delta\Delta G_{ex}$ values of the residues belonging to the domain's core, which need large structural disruptions with high enthalpies and entropies to become exposed to the solvent [22,23],

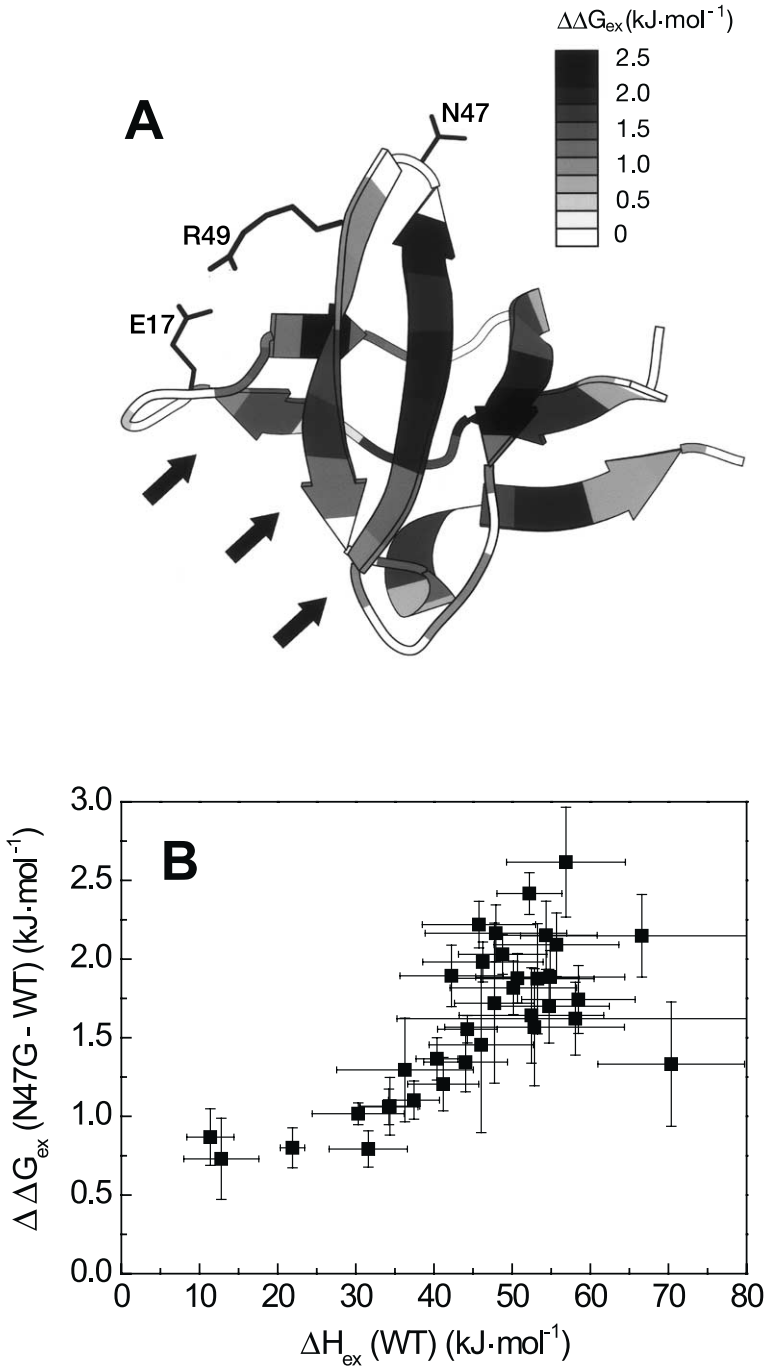

Fig. 3. A: Schematic representation of the SH3 crystal structure showing in grey-scale code (from 0 to 2.5 kJ/mol) the increment in apparent Gibbs energy of HX, $\Delta\Delta G_{ex}$, produced by the mutation N47G at pH 3.0 and 27.1°C. Residues for which $\Delta\Delta G_{ex}$ could not be determined are represented in white. The black arrows indicate the location of the binding site for proline-rich peptides. The side chains of Asn47, Glu17 and Arg49 are represented by black sticks. The figure was made with MOLSCRIPT [33]. B: Plot of the $\Delta\Delta G_{ex}$ values at pH 3.0 and 27.1°C corresponding to the N47G mutation versus the average enthalpy of HX, ΔH_{ex}, for WT SH3 under the same conditions. The ΔH_{ex} data were taken from [23].

are on the whole similar to $\Delta\Delta G_{unf}$. This means that the sub-ensemble of states exposing each core residue is on average destabilised in a similar way to the unfolded state, which indicates that the native interactions modified by the N47G mutation are no longer present in most of the states of these sub-ensembles, i.e. the distal loop is disrupted. This is particularly important in that the HX of most residues in the core of the SH3 domain does not occur by global unfolding alone but is mainly governed by Gibbs energy states that are significantly lower than the globally unfolded state [9]. These states appear however to be largely unstructured, as we have proposed recently [22,23]. Our results here support the proposal that native HX in proteins occurs via a wide distribution of conformational fluctuations extending even above the transition state barrier of folding [32].

Other residues, mainly in the loops and chain ends, have lower but significant $\Delta\Delta G_{ex}$ values. For example, residues exchanging via low-energy states, such as Leu8, Gln16, Thr24,

Thr37, Lys60 or Leu61, with $\Delta G_{ex} < 6$ kJ/mol, still show $\Delta\Delta G_{ex}$ values near 1 kJ/mol and higher. This suggests that a fraction of the sub-ensembles by which these residues exchange have a distorted distal loop. This kind of state might occur for example via simultaneous local unfoldings in the region of the residue in question and also in the distal loop. The probability of this kind of state may be increased as the result of a cooperative pathway connecting the two regions. As the statistical weight of these states is also reduced by the mutation, this results in significant $\Delta\Delta G_{ex}$ values and thus in the stabilisation of these flexible regions by the mutation. This has been proposed as the molecular basis for long-range cooperative effects in proteins [12,13]. Despite the fact that the mutation in the distal loop has quite a small effect upon the rest of the native structure, there is an energetic cooperative link between the distal loop and other discrete flexible regions of the small domain. This appears to manifest itself in the binding site for the p41 peptide with a reduction of the affinity produced by the mutations.

Acknowledgements: We thank Dr. Luis Serrano for kindly providing the plasmid encoding the SH3 domains. We acknowledge the technical help in the NMR experiments of Dr. A. Haidour of the CIC of the University of Granada. We also thank our colleague Dr. J. Trout for revising the English text. This work was financed by grants PL96-2180 from the European Union and BIO2000-1459 from the Spanish Ministry of Science and Technology. S.C. acknowledges a pre-doctoral fellowship from the Andalucian Regional Government.

References

[1] Jeng, M.-F. and Englander, S.W. (1991) J. Mol. Biol. 221, 1045–1061.
[2] Radford, S.E., Buck, M., Topping, K.D., Dobson, C.M. and Evans, P.A. (1992) Proteins 14, 237–248.
[3] Woodward, C. (1993) Trends Biochem. Sci. 18, 359–360.
[4] Clarke, J. and Fersht, A.R. (1996) Fold. Des. 1, 243–254.
[5] Swint-Kruse, L. and Robertson, A.D. (1996) Biochemistry 35, 171–180.
[6] Bai, Y., Sosnick, T.R., Mayne, L. and Englander, S.W. (1995) Science 269, 192–197.
[7] Morozova, L.A., Haynie, D.T., Arico-Muendel, C., Van Dael, H. and Dobson, C.M. (1995) Nat. Struct. Biol. 2, 871–875.
[8] Chamberlain, A.K. and Marqusee, S. (1998) Biochemistry 37, 1736–1742.
[9] Sadqi, M., Casares, S., Abril, M.A., López-Mayorga, O., Conejero-Lara, F. and Freire, E. (1999) Biochemistry 38, 8899–8906.
[10] Englander, S.W. (2000) Annu. Rev. Biophys. Biomol. Struct. 29, 213–238.
[11] Hilser, J.V., Dowdy, D., Oas, T.G. and Freire, E. (1998) Proc. Natl. Acad. Sci. USA 95, 9903–9908.
[12] Freire, E. (2000) Proc. Natl. Acad. Sci. USA 97, 11680–11682.
[13] Pan, H., Lee, J.C. and Hilser, V.J. (2000) Proc. Natl. Acad. Sci. USA 97, 12020–12025.
[14] Luque, I., Leavitt, S.A. and Freire, E. (2002) Annu. Rev. Biophys. Biomol. Struct. 31, 235–256.
[15] Kuriyan, J. and Cowburn, D. (1993) Curr. Opin. Struct. Biol. 3, 828–837.
[16] Viguera, A.R., Martinez, J.C., Filimonov, V.V., Mateo, P.L. and Serrano, L. (1994) Biochemistry 33, 2142–2150.
[17] Martínez, J.C., Pisabarro, M.T. and Serrano, L. (1998) Nat. Struct. Biol. 5, 721–729.
[18] Martínez, J.C. and Serrano, L. (1999) Nat. Struct. Biol. 6, 1010–1016.
[19] Grantcharova, V.P., Riddle, D.S., Santiago, J.V. and Baker, D. (1998) Nat. Struct. Biol. 5, 714–720.
[20] Vega, M.C., Martínez, J.C. and Serrano, L. (2000) Protein Sci. 9, 2322–2328.
[21] Musacchio, A., Noble, M., Pauptit, R., Wierenga, R. and Saraste, M. (1992) Nature 359, 851–855.
[22] Sadqi, M., Casares, S., López-Mayorga, O., Martínez, J.C. and Conejero-Lara, F. (2002) FEBS Lett. 514, 295–299.
[23] Sadqi, M., Casares, S., López-Mayorga, O. and Conejero-Lara, F. (2002) FEBS Lett. 527, 86–90.
[24] Higuchi, R., Krummel, B. and Saiki, R.K. (1988) Nucleic Acids Res. 16, 7351–7367.
[25] Pisabarro, M. and Serrano, L. (1996) Biochemistry 35, 10634–10640.
[26] Delaglio, F., Grzesiek, S., Vuister, G.W., Zhu, G., Pfeifer, J. and Bax, A. (1995) J. Biomol. NMR 6, 277–293.
[27] Johnson, B.A. and Blevins, R.A. (1994) J. Biomol. NMR 4, 603–614.
[28] Bai, Y., Milne, J.S., Mayne, L. and Englander, S.W. (1993) Proteins 17, 75–86.
[29] Vriend, G. (1990) J. Mol. Graph. 8, 52–56.
[30] Hilser, J.V. and Freire, E. (1996) J. Mol. Biol. 262, 756–772.
[31] Hilser, J.V. and Freire, E. (1997) Proteins 27, 171–183.
[32] Parker, M.J. and Marqusee, S. (2000) J. Mol. Biol. 300, 1361–1375.
[33] Kraulis, P.J. (1991) J. Appl. Crystallogr. 24, 946–950.